**Zika virus infection drives epigenetic modulation of immunity by the histone acetyltransferase CBP of *Aedes aegypti***

Anderson de Mendonça Amarante[1,2], Isabel Caetano de Abreu da Silva[1,2], Vitor Coutinho Carneiro[3,] Amanda Roberta Revoredo Vicentino[1,] Marcia de Amorim Pinto[1], Luiza Mendonça Higa[4], Kanhu Charan Moharana[5], Octávio Augusto C. Talyuli[1,2], Thiago Motta Venancio[2,5], Pedro Lagerblad de Oliveira[1,2], and Marcelo Rosado Fantappié[1,2]*

[1]Instituto de Bioquímica Médica Leopoldo de Meis, Programa de Biologia Molecular e Biotecnologia, Centro de Ciências da Saúde, 21941-902, Universidade Federal do Rio de Janeiro, Rio de Janeiro, Brasil;

[2]Instituto Nacional de Entomologia Molecular, 21941-902, Universidade Federal do Rio de Janeiro, Rio de Janeiro, Brasil;

[3]Division of Epigenetics, German Cancer Research Center, Im Neuenheimer Feld 580, 69120 Heidelberg, Germany;

[4]Departamento de Genética, Instituto de Biologia, Universidade Federal do Rio de Janeiro, Rio de Janeiro, RJ, 21941-617, Brasil;

[5]Laboratório de Química e Função de Proteínas e Peptídeos, Centro de Biociências e Biotecnologia, Universidade Estadual do Norte Fluminense Darcy Ribeiro, Campos dos Goytacazes, 28013-602, Brasil.

*Corresponding author: M.R. Fantappié, Instituto de Bioquímica Médica, Universidade Federal do Rio de Janeiro, CCS, Ilha do Fundão, Rio de Janeiro, 21941-902, Brasil. Tel: +55-21-3938-6608; E-mail: fantappie@bioqmed.ufrj.br

Keywords: *Aedes aegypti*, Zika, chromatin, epigenetics, histone acetylation, immunity.

## Abstract

Epigenetic mechanisms are responsible for a wide range of biological phenomena in insects, controlling embryonic development, growth, aging and nutrition. Despite this, the role of epigenetics in shaping insect-pathogen interactions has received little attention. Gene expression in eukaryotes is regulated by histone acetylation/deacetylation, an epigenetic process mediated by histone acetyltransferases (HATs) and histone deacetylases (HDACs). In this study, we explored the role of the *Aedes aegypti* histone acetyltransferase CBP (AaCBP) after infection with Zika virus (ZIKV), focusing on the two main immune tissues, the midgut and fat body. We showed that the expression and activity of AaCBP could be positively modulated by blood meal and ZIKV infection. Nevertheless, Zika-infected mosquitoes that were silenced for *AaCBP* revealed a significant reduction in the acetylation of H3K27 (CBP target marker), followed by downmodulation of the expression of immune genes, higher titers of ZIKV and lower survival rates. Importantly, in Zika-infected mosquitoes that were treated with sodium butyrate, a histone deacetylase inhibitor, their capacity to fight virus infection tends to be rescued. Our data point to a direct correlation among histone hyperacetylation by AaCBP, upregulation of antimicrobial peptide genes and increased survival of Zika-infected-*A. aegypti*.

**Author summary**

Pathogens have coevolved with mosquitoes to optimize transmission to hosts. As natural vectors, mosquitoes are permissive to and allow systemic and persistent arbovirus infection, which intriguingly does not result in dramatic pathological sequelae that affect their lifespan. In this regard, mosquitoes have evolved mechanisms to tolerate persistent infection and develop efficient antiviral strategies to restrict viral replication to nonpathogenic levels. There is a great deal of evidence supporting the implication of epigenetics in the modulation of the biological interaction between hosts and pathogens. This study reveals that Zika virus infection positively modulates the expression and activity of *A. aegypti* histone acetyltransferase CBP (AaCBP). This study shows that AaCBP plays a role in the activation of immune-responsive genes to limit Zika virus replication. This first description that Zika virus infection has epigenomic consequences in the regulation of *A. aegypti* immunity opens a new avenue for research on mosquito factors that can drive vector competence.

## Introduction

Mosquitoes are primary vectors of a variety of human pathogens throughout the world. *Aedes aegypti* mosquitoes can develop long-lasting viral infections and carry high viral loads, which make them efficient vectors for the transmission of arboviruses such as Zika virus (ZIKV) (Weaver et al., 2016).

Host-pathogen interactions are among the most plastic and dynamic systems in nature. In this regard, epigenetic modifications can offer an accessory source of fast-acting, reversible and readily available phenotypic variation that can be directly

shaped by both host and pathogen selection pressures(Gómez-Díaz et al., 2012; Ruiz et al., 2019). One of the hallmarks in the study of host gene regulation is to elucidate how specific sets of genes are selected for expression in response to pathogen infection.

Understanding the interactions between the mosquito immune system and viruses is critical for the development of effective control strategies against these diseases. Mosquitoes have conserved immune pathways that limit infections by viral pathogens (Angleró-Rodríguez et al., 2017; Tikhe & Dimopoulos, 2021). Mosquito antiviral defense is regulated by RNA interference (RNAi), Janus kinase/signal transducer (JAK-STAT), Toll, the immune deficiency (IMD) and MAPK immune pathways (Angleró-Rodríguez et al., 2017; Asad et al., 2018; Tikhe & Dimopoulos, 2021).

The Toll pathway has been shown to play the most important role in controlling ZIKV infections (Angleró-Rodríguez et al., 2017). In this context, gene expression analysis of ZIKV-infected mosquitoes has indicated that Toll pathway-related genes are highly upregulated in Zika infection when compared to other immune pathways (Angleró-Rodríguez et al., 2017; Tikhe & Dimopoulos, 2021).

Eukaryotic gene expression is controlled by the functions of *cis*-DNA elements, enhancers and promoters, which are bound by transcription factors, in combination with the organization of the chromatin (Barrera & Ren, 2006). Although it is still poorly understood how chromatin-associated processes participate in the regulation of gene transcription in the context of pathogen-vector interactions, it has been previously shown that *Plasmodium falciparum* infection induces significant chromatin changes in the *Anopheles gambiae* mosquitoes (Ruiz et al., 2019). This

study identified infection-responsive genes showing differential enrichment in various histone modifications at the promoter sites (Ruiz et al., 2019).

The transcriptional coactivator CREB-binding protein (CBP), and its paralog p300, play a central role in coordinating and integrating multiple signal-dependent events with the transcription apparatus, allowing the appropriate level of gene activity to occur in response to diverse stimuli (Chan & Thangue, 2001). CBP proteins do not specifically interact with the promoter elements of target genes, but they are recruited to promoters by interaction with DNA-bound transcription factors, which directly interact with the RNA polymerase II complex (Chan & Thangue, 2001; Revilla & Granja, 2009). A key property of CBP is the presence of histone acetyltransferase (HAT) activity, which endows the enzyme with the capacity to influence chromatin activity by the acetylation of histones (Chan & Thangue, 2001).

Consistent with its function as a transcriptional coactivator, CBP plays crucial roles in embryogenesis (Fang et al., 2014), development (Bantignies et al., 2002), differentiation (Bantignies et al., 2002; Fauquier et al., 2018), oncogenesis (Bantignies et al., 2002; Iyer et al., 2004) and immunity (Revilla & Granja, 2009). Although most of these studies have been conducted in mammalian systems, nonvector insect models have also made important contributions to the biological functions of CBP (Kirfel et al., 2020; Li et al., 2018; Sedkov et al., 2003; Tie et al., 2009).

The present work describes the functional characterization of a histone acetyltransferase in an insect vector and provides indications that Zika virus infection exerts epigenomic consequences in regulating *A. aegypti* immunity.

## Materials and Methods

### Ethics statement

All animal care and experimental protocols were conducted in accordance with the guidelines of the Committee for Evaluation of Animal Use for Research – CEUA of the Federal University of Rio de Janeiro (UFRJ). The protocols were approved by CEUA-UFRJ under the registration number IBQM149/19. Technicians in the animal facility at the Instituto de Bioquímica Médica Leopoldo de Meis (UFRJ) carried out all protocols related to rabbit husbandry under strict guidelines to ensure careful and consistent animal handling.

### Mosquito rearing and cell culture

*Aedes aegypti* (*Liverpool black-eyed* strain) were raised in a mosquito rearing facility at the Federal University of Rio de Janeiro, Brazil, under a 12-h light/dark cycle at 28 $^{o}$C and 70-80% relative humidity. Larvae were fed dog chow, and adults were maintained in a cage and given a solution of 10% sucrose *ad libitum*. Females 7-10 days posteclosion were used in the experiments. When mentioned, mosquitoes were artificially fed heparinized rabbit blood. For virus infection, mosquitoes were fed using water-jacketed artificial feeders maintained at 37 $^{o}$C sealed with parafilm membranes. Alternatively, mosquitoes were infected by intrathoracic injections of 69 nL containing 60 Plaque Forming Units (PFUs) of ZIKV.

Female midguts or fat bodies were dissected 24, 48, 72 or 96 h after feeding for RNA sample preparation.

The *A. aegypti* embryonic cell line Aag2 was maintained in Schneider medium (Merk) supplemented with 5% FBS (LGC, Brazil) and 1% penicillin/streptomycin/amphotericin B. Aag2 cells were incubated at 28 $^{o}$C.

ZIKV infection and virus titration

ZIKV strain Pernambuco (ZIKV strain ZIKV/H.sapiens/Brazil/PE243/201) (Donald et al., 2016) was propagated in the *A. albobictus* C6/36 cell line, and titers were determined by plaque assay on Vero cells. ZIKV was propagated in C6/36 cells for 6-8 days; virus was then harvested, filtered through 0.22 and 0.1μm membranes, respectively and stored at -80 $^{o}$C. Mosquitoes were intrathoracically infected by microinjections (Göertz et al., 2019) of 69 nL of virus, containing 60 PFUs.

Midguts and fat bodies were dissected, individually collected, and stored at –80 $^{o}$C until use for plaque assays. Virus titration was performed as described previously (Sim et al., 2013). Plates were incubated for 4-5 days, fixed and stained with a methanol/acetone and 1% crystal violet mixture, and washed, after which the plaque forming units (PFUs) were counted.

AaCBP gene knockdown by RNAi

Double-stranded RNA (dsRNA) was synthesized from templates amplified from cDNA of adult female mosquitoes using specific primers containing a T7 tail (Supplementary Table 1). The *in vitro* dsRNA transcription reaction was performed following the manufacturer's instructions (Ambion MEGAscript RNAi). Two different dsRNA products (dsAaCBP1 and dsAaCBP2) were PCR amplified based on

the coding sequence of *A. aegypti* CBP (GenBank accession number XP_011493407.2), using the oligonucleotides listed in Supplementary Table 1. The irrelevant control gene luciferase (dsLuc) was amplified from the luciferase T7 control plasmid (Promega). Female mosquitoes were injected intrathoracically (Ramirez et al., 2012) with dsRNA (0.4 μg) with a microinjector (NanoJect II Autonanoliter injector, Drummond Scientific, USA). Injected mosquitoes were maintained at 28 $^{o}$C, and 70-80% humidity, with 10% sucrose provided *ad libitum*.

RNA isolation and quantitative real-time PCR

Total RNA was isolated from whole bodies, midguts or fat bodies of adult females, using the RiboPure kit (Ambion) followed by DNase treatment (Ambion) and cDNA synthesis (SuperScript III First-Strand Synthesis System, Invitrogen), following the manufacturer's instructions. Quantitative reverse transcription gene amplifications (qRT-PCR) were performed with StepOnePlus Real-Time PCR System (Applied Biosystems) using the Power SYBR Green PCR Master Mix (Applied Biosystems). The comparative *Ct* method (Livak & Schmittgen, 2001) was used to compare mRNA abundance. In all qRT-PCR analyses, the *A. aegypti* ribosomal protein 49 gene (*Rp*49) was used as an endogenous control (Gentile et al., 2005). All oligonucleotide sequences used in qRT-PCR assays are listed in the Supplementary Table 1.

## Western blotting

Protein extracts were prepared as previously described (Coutinho Carneiro et al., 2020; Ribeiro et al., 2012). Briefly, *A. aegypti* total protein extracts were carried out by homogenizing adult female mosquitoes or Aag2 cells in TBS containing a protease inhibitor cocktail (Sigma). Proteins were recovered from the supernatant by centrifugation at 14.000xg, for 15 min. at 4 $^{o}$C. Protein concentration was determined by the Bradford Protein Assay (Bio-Rad). Western blots were carried out using secondary antibody (Immunopure goat anti-mouse, #31430). The primary monoclonal antibodies (ChIP grade) used were anti-H3 pan acetylated (Sigma-Aldrich #06-599), anti-H3K9ac (Cell Signaling Technology #9649) and Anti-H3K27ac (Cell Signaling Technology, #8173), according to the manufacture's instructions. For all antibodies, a 1:1000 dilution was used. For normalization of the signals across the samples, an anti-histone H3 antibody (Cell Signaling Technology, #14269) was used.

## Statistical analysis

All analyses were performed with the GraphPad Prism statistical software package (Prism version 6.0, GraphPad Software, Inc., La Jolla, CA). *Asterisks* indicate significant differences (*, $p < 0.05$; **, $p < 0.01$; ***, $p < 0.001$; ns, not significant).

Genome-wide identification of lysine acetyltransferases in *A. aegypti*

We obtained the latest *A. aegypti* proteome and functional annotations (AaegL5.0) from NCBI RefSeq (https://ftp.ncbi.nlm.nih.gov/genomes/all/GCF/002/204/515/GCF_002204515.2_AaegL5.0). The amino acid sequences of the 23 *D. melanogaster* lysine acetyltransferases (DmKATs) reported by Feller *et al* 2015 were obtained from FlyBase. The KAT orthologs in *A. aegypti* were identified using BlastP (e-value ≤1e-10, identity ≥25% and query coverage ≥50%) (Altschul et al., 1997). We further validated the presence of various acetyltransferase domains in these KATs. Conserved domains were predicted in putative KATs using hmmer (e-value ≤ 0.01; http://hmmer.org/) and the PFAM-A database. Following the nomenclature of DmKATs and the conserved domain architectures, AeKATs were classified into 5 major sub-families: HAT1, Tip60, MOF, HBO1, GCN5 and CBP (Feller et al., 2015). Conserved domain architectures were rendered with DOG (Domain Graph, version 1.0) (Ren et al., 2009). Multiple sequence alignment of AeKATs was performed using using Clustalw (Thompson et al., 1994).

## Results

*Aedes aegypti* has an ortholog of the CREB-binding protein (CBP) and five additional putative histone acetyltransferases

The *A. aegypti* transcriptional coactivator CBP (AaCBP) contains all five canonical structural and functional domains (Fig 1) of the CBP family (Liu et al., 2008). The TAZ, KIX and CREB are the protein interaction domains that mediate

interactions with transcription factors. The histone acetyltransferase (HAT) catalytic domain of the CBP enzymes shows high level of conservation among different species (Fig 1), as well as among other HATs from *A. aegypti* (Supplementary Fig 1A and B). AaCBP also contains a bromo domain, which binds acetylated lysines. The conserved domains are connected by long stretches of unstructured linkers.

Because transcriptional coactivator complexes are intricate structures composed of multiple subunits, and because cooperative assembly of histone acetyltransferases is a rate-limiting step in transcription activation, we aimed to identify other HATs in *A. aegypti*. By searching the latest *A. aegypti* proteome and functional annotations (see Methods), we identified six other putative HATs, all containing the conserved HAT functional domain (Supplementary Fig 1A and B).

ZIKV infection modulates the expression and activity of AaCBP

Mosquitoes naturally acquire viral infections when they feed on blood. In this context, it is well established that in addition to extensive genome-wide transcriptional modulation in mosquitoes after blood meals (Bonizzoni et al., 2011), viral infections can also modulate host cell gene expression and influence cellular function. Thus, we first evaluated whether a blood meal was able to modulate the expression of AaCBP in the midgut or fat body (Supplementary Fig 2). We showed that the expression of AaCBP in both tissues was significantly upregulated by blood meal, reaching its peak of transcription at 24 and 48 h after feeding (Supplementary Fig 2A and B). The stimulated transcription of AaCBP was especially dramatic in the fat body 48 h after a blood meal (Supplementary Fig 2B). Because we were particularly interested in evaluating the functional role of AaCBP in ZIKV infection,

we were forced to change our virus infection approach. As an alternative to feeding infected blood, mosquitoes were infected with ZIKV by intrathoracic injections. Importantly, we showed that ZIKV infection was also able to upregulate the expression of AaCBP in the midgut or fat body, reaching its peak transcription at four days after infection (Fig 2A and B). However, we did not see upregulation when we assayed head and thorax (Fig 2C). A similar phenomenon was observed when we used Aag2 cells, where the expression of AaCBP reached their peaks at 6 and 15 h, post infection, respectively (Fig 2 D). Importantly, we confirmed that the increase in mRNA expression correlated with the increase in AaCBP acetylation activity (Fig 2 E and F). Of note, ZIKV infection enhanced the acetylation activity of AaCBP toward lysine 27 of histone H3 (H3K27ac), but not toward lysine 9 of histone H3 (H3K9ac), (Fig 2F). Considering that H3K27 is the main target substrate for CBP enzymes (Raisner et al., 2018), and that H3K9 is the main substrate of Gcn5 HAT (Karmodiya et al., 2012) (also present in *A. aegypti*; see Supplementary Fig 1A and B), these results point to a specific enhancement of AaCBP by ZIKV infection.

AaCBP plays a role in the defense and survival of ZIKV-infected mosquitoes

To investigate the role of AaCBP in the lifespan of mosquitoes infected with ZIKV, we knocked down the *AaCBP* gene two days before infection and followed their survival rates for 20 days, on a daily basis (Fig 3A). It is important to emphasize that it was mandatory to use intrathoracic injections for ZIKV infection in these experiments. This was due to the fact that *AaCBP* gene silencing was not successfully achieved when a blood meal was utilized (Supplementary Fig 3; of note, we showed that the expression of AaCBP is upregulated by blood meal, and thus, this likely

counteracted the effects of the silencing). The levels of silencing of AaCBP at Day 2 post dsRNA injections were 50% in the midgut and 80% in the fat body, as judged by its mRNA expression and activity (Supplementary Fig 4A and B). Mock-infected mosquitoes that received dsLuc injections, showed a high rate of survival until Day 15, when survival started to decline, most likely due to normal aging (Fig 3B, black lines. Mock-infected mosquitoes that were silenced for AaCBP revealed a mortality rate of 60% at Day 20 (Fig 3B, blue line), a similar pattern observed for ZIKV-infected mosquitoes that received injections with the dsLuc control (Fig 3B, green line). Importantly, mosquitoes that were silenced for AaCBP followed by ZIKV infections showed a much higher mortality rate than all other groups (Fig 3B, orange line). These results clearly show that even a partial deletion of AaCBP is enough to disrupt the homeostasis of the mosquito (Fig 3B blue line), and when virus infection occurs, the lack of AaCBP becomes enormously detrimental.

To correlate the lack of AaCBP and mortality, with an increase in viral loads, we determined viral titers over time in the midguts and fat bodies (Fig 3C and D, respectively). We clearly saw that AaCBP-silenced mosquitoes did not efficiently fight virus infections in these tissues that are expected to mount strong immune responses against viruses (Angleró-Rodríguez et al., 2017; Cheng et al., 2016; Tikhe & Dimopoulos, 2021). In this respect, our data reconfirmed that antimicrobial peptides (AMPs) are highly upregulated by ZIKV infections in the midgut (Supplementary Fig 5).

AaCBP regulates the expression of antiviral immune-response genes

Because AaCBP-silenced mosquitoes revealed higher viral loads than control-silenced mosquitoes (Fig 3C and D), and knowing the transcriptional coactivator role of CBP enzymes, we questioned whether AaCBP knockdown could have affected the transcription of antiviral immune-response genes. Indeed, qRT-PCR analysis showed that the lack of AaCBP led to downregulation of the immune-response genes *cecropin D, cecropin G, and defensin C,* in the midgut or fat body (Fig 4A and B, respectively). In addition, the *vago 2* gene was also downregulated in the fat body (Fig 4B). Interestingly, *vago 2* has been shown to be upregulated in *A. aegypti* larvae exposed to dengue virus (DENV) (Vargas et al., 2020), as well as in *A. albopictus* cells infected with DENV (Paradkar et al., 2014). Of note, two members of the RNAi (*si*RNA) pathway, dicer 2 and Ago 2 were not modulated in either tissue of AaCBP-silenced mosquitoes (Fig 4A and B). Importantly, downregulation of antiviral immune-response genes persisted until at least day five-post infection, which matched the kinetics of AaCBP-mediated gene silencing (Supplementary Fig 6A-D).

Histone hyperacetylation induces mosquito immune responses and suppression of ZIKV infection

Histone deacetylation by histone deacetylases (HDACs) is involved in chromatin compaction and gene repression (Shahbazian & Grunstein, 2007). Inhibition of HDACs by sodium butyrate (NaB) leads to histone hyperacetylation and potent gene activation (Kurdistani & Grunstein, 2003). We treated mosquitoes with NaB and showed a significant increase in H3K27 and H3K9 acetylation

(Supplementary Fig 7A and B). An increase in total histone H3 acetylation could not be observed (Supplementary Fig 7A and B), which is somehow expected if one considers that a combination of acetylated and nonacetylated H3 might coexist in a specific cell type and/or during a specific period. We next investigated the effect of NaB in ZIKV-infected mosquitoes (Fig 5) and showed that the expression levels of defensin A, defensin C and cecropin D were significantly increased (Fig 5A-C). Importantly, the effect of NaB treatment consisten tly showed a tendency for a reduction in viral loads (Fig 5D and E)**.** It is important to emphasize that NaB treatment leads to hyperacetylation of all histones. In this respect, we observed hyperacetylation of H3K27, (a CBP target) and H3K9 (a Gcn5 target). However, the acetylation levels of H3K27 were higher than those of H3K9 (Supplementary Fig 7A and B), likely due to the specific enhancement of AaCBP gene expression and activity by ZIKV infection (Fig 2), which was not observed for AaGcn5 activity (Fig 2F, H3K9ac panel). All together, these data suggest a direct correlation between high chromatin decompaction, AMPs overexpression, and strong immunity.

## Discussion

Upon pathogen detection, the innate immune system must be able to mount a robust and quick response, but equally important is the need to rein in the cytotoxic effects of such a response. Immune-response genes are maintained in a silent, yet poised, state that can be readily induced in response to a particular pathogen, and this characteristic pattern is achieved through the action of two elements: the activation of transcription factors and the modulation of the chromatin environment at gene promoters. Although the activation route of the immune pathways against viruses is

relatively well known in *A. aegypti*, our work is the first to attempt to explore the role of chromatin structure in this process.

The regulation of cellular functions by gene activation is accomplished partially by acetylation of histone proteins to open the chromatin conformation, and strikingly, CBP histone acetyltransferase activity always plays a role in this process (Dancy & Cole, 2015). One example of signals that ultimately use CBP enzymes as transcriptional coregulators includes the NF-*k*B signaling (Mukherjee et al., 2013).

*CBP* genes are conserved in a variety of multicellular organisms, from worms to humans and play a central role in coordinating and integrating multiple cell signal-dependent events. In this regard, the *A. aegypti* CBP shows a high degree of homology, notably within the functional domains, with well-characterized human and fly enzymes (Fig 1). Therefore, one might anticipate that AaCBP functions as a transcriptional coactivator in a variety of physiological processes of the mosquito, including innate immunity.

The Toll pathway is an NF-*k*B pathway that plays an important role in immunity in mosquitoes (Angleró-Rodríguez et al., 2017; Cheng et al., 2016; Tikhe & Dimopoulos, 2021). Gene expression analysis of ZIKV-infected mosquitoes has shown that Toll pathway-related genes are highly upregulated in ZIKV infection when compared to other immune pathways (Angleró-Rodríguez et al., 2017). Here, we showed that the expression of AaCBP is also upregulated upon ZIKV infection and that CBP-dependent histone acetylation enables the mosquito to fight viral infections. Although it is not yet clear how AaCBP could limit virus replication, one could envision a molecular role where a particular transcription factor (for example, Rel1) would recruit AaCBP to immune-related gene (for example, AMP genes) promoters and/or enhancers and acetylate histones (for example, H3K27), culminating

with chromatin decompaction and gene activation (depicted in our hypothetical model in Fig 6). Indeed, we experimentally demonstrated in part that our model might be correct: 1. We showed that ZIKV-infection potentiates AaCBP-mediated H3K27 acetylation (a mark of gene activation); 2. The lack of AaCBP leads to downregulation of immune-related genes, higher loads of ZIKV virus, and lower rates of mosquito survival; 3. An inverse phenotype was obtained under H3K27 hyperacetylation. Nevertheless, the AaCBP-bound transcription factor in this signaling pathway has yet to be determined.

Host-pathogen interactions provide a highly plastic and dynamic biological system. To cope with the selective constraints imposed by their hosts, many pathogens have evolved unparalleled levels of phenotypic plasticity in their life history traits (Reece et al., 2009). Likewise, the host phenotype is drastically and rapidly altered by the presence of a pathogen (Edelaar et al., 2021; Rando & Verstrepen, 2007). One important example of these alterations is the manipulative strategy of the pathogen aimed at maximizing its survival and transmission, and one obvious target is the host's immune system. In recent years, the epigenetic modulation of the host's transcriptional program linked to host defense has emerged as a relatively common occurrence of pathogenic viral infections (Paschos & Allday, 2010). Interestingly and importantly, our data reveal that chromatin remodeling by histone acetylation contributes to establishing a resistance in ZIKV-infected *A. aegypti*. In this respect, we showed that ZIKV-infected wild type *A. aegypti* resisted to infections better than ZIKV-infected-AaCBP-silenced mosquitoes, whose survival was drastically compromised (Fig 3B). Thus, our data point to an important role of AaCBP in maintaining *A. aegypti* homeostasis through fine-tuning the transcriptional control of immune genes.

Our work has attempted to explore the epigenetic nature of virus-vector interactions. We have focused on epigenetic events that initiate changes in the vector nucleus, likely involving the cooperation between transcription factors and chromatin modifiers to integrate and initiate genomic events, which culminate with the limitation of Zika virus replication.

**References**


Altschul, S. F., Madden, T. L., Schäffer, A. A., Zhang, J., Zhang, Z., Miller, W., & Lipman, D. J. (1997). Gapped BLAST and PSI-BLAST: a new generation of protein database search programs. *Nucleic Acids Research*, *25*(17), 3389–3402. https://doi.org/10.1093/nar/25.17.3389

Angleró-Rodríguez, Y. I., MacLeod, H. J., Kang, S., Carlson, J. S., Jupatanakul, N., & Dimopoulos, G. (2017). Aedes aegypti Molecular Responses to Zika Virus: Modulation of Infection by the Toll and Jak/Stat Immune Pathways and Virus Host Factors. *Frontiers in Microbiology*, *8*, 2050. https://doi.org/10.3389/fmicb.2017.02050

Asad, S., Parry, R., & Asgari, S. (2018). Upregulation of Aedes aegypti Vago1 by Wolbachia and its effect on dengue virus replication. *Insect Biochemistry and Molecular Biology*, *92*, 45–52. https://doi.org/10.1016/j.ibmb.2017.11.008

Bantignies, F., Goodman, R. H., & Smolik, S. M. (2002). The interaction between the coactivator dCBP and Modulo, a chromatin-associated factor, affects segmentation and melanotic tumor formation in Drosophila. *Proceedings of the National Academy of Sciences of the United States of America*, *99*(5), 2895–2900. https://doi.org/10.1073/pnas.052509799

Barrera, L. O., & Ren, B. (2006). The transcriptional regulatory code of eukaryotic cells – insights from genome-wide analysis of chromatin organization and transcription factor binding. *Current Opinion in Cell Biology*, *18*(3), 291–298. https://doi.org/https://doi.org/10.1016/j.ceb.2006.04.002

Bonizzoni, M., Dunn, W. A., Campbell, C. L., Olson, K. E., Dimon, M. T., Marinotti, O., & James, A. A. (2011). RNA-seq analyses of blood-induced changes in gene expression in the mosquito vector species, Aedes aegypti. *BMC Genomics*, *12*(1), 82. https://doi.org/10.1186/1471-2164-12-82

Chan, H. M., & Thangue, N. B. La. (2001). *p300 / CBP proteins : HATs for transcriptional bridges and scaffolds*. J Cell Sci.;114(Pt 13):2363-73. PMID: 11559745

Cheng, G., Liu, Y., Wang, P., & Xiao, X. (2016). Mosquito Defense Strategies against Viral Infection. *Trends in Parasitology*. https://doi.org/10.1016/j.pt.2015.09.009

Coutinho Carneiro, V., de Abreu da Silva, I. C., Amaral, M. S., Pereira, A. S. A., Silveira, G. O., Pires, D. da S., Verjovski-Almeida, S., Dekker, F. J., Rotili, D., Mai, A., Lopes-Torres, E. J., Robaa, D., Sippl, W., Pierce, R. J., Borrello, M. T., Ganesan, A., Lancelot, J., Thiengo, S., Fernandez, M. A., … Fantappié, M. R. (2020). Pharmacological inhibition of lysine-specific demethylase 1 (LSD1) induces global transcriptional deregulation and ultrastructural alterations that impair viability in Schistosoma mansoni. *PLoS Neglected Tropical Diseases*, *14*(7), e0008332. https://doi.org/10.1371/journal.pntd.0008332

Dancy, B. M., & Cole, P. A. (2015). Protein lysine acetylation by p300/CBP. *Chemical Reviews*, *115*(6), 2419–2452. https://doi.org/10.1021/cr500452k

Donald, C. L., Brennan, B., Cumberworth, S. L., Rezelj, V. V., Clark, J. J., Cordeiro,

M. T., Freitas de Oliveira França, R., Pena, L. J., Wilkie, G. S., Da Silva Filipe, A., Davis, C., Hughes, J., Varjak, M., Selinger, M., Zuvanov, L., Owsianka, A. M., Patel, A. H., McLauchlan, J., Lindenbach, B. D., … Kohl, A. (2016). Full Genome Sequence and sfRNA Interferon Antagonist Activity of Zika Virus from Recife, Brazil. *PLoS Neglected Tropical Diseases*, *10*(10), 1–20. https://doi.org/10.1371/journal.pntd.0005048

Edelaar, P., Bonduriansky, R., Charmantier, A., Danchin, E., & Pujol, B. (2021). Response to Kalchhauser et al.: Inherited Gene Regulation Is not Enough to Understand Nongenetic Inheritance. In *Trends in ecology & evolution* (Vol. 36, Issue 6, pp. 475–476). https://doi.org/10.1016/j.tree.2021.03.002

Fang, F., Xu, Y., Chew, K.-K., Chen, X., Ng, H.-H., & Matsudaira, P. (2014). Coactivators p300 and CBP maintain the identity of mouse embryonic stem cells by mediating long-range chromatin structure. *Stem Cells (Dayton, Ohio)*, *32*(7), 1805–1816. https://doi.org/10.1002/stem.1705

Fauquier, L., Azzag, K., Parra, M. A. M., Quillien, A., Boulet, M., Diouf, S., Carnac, G., Waltzer, L., Gronemeyer, H., & Vandel, L. (2018). CBP and P300 regulate distinct gene networks required for human primary myoblast differentiation and muscle integrity. *Scientific Reports*, *8*(1), 12629. https://doi.org/10.1038/s41598-018-31102-4

Feller, C., Forné, I., Imhof, A., & Becker, P. B. (2015). Global and specific responses of the histone acetylome to systematic perturbation. *Molecular Cell*, *57*(3), 559–571. https://doi.org/10.1016/j.molcel.2014.12.008

Gentile, C., Lima, J. B. P., & Peixoto, A. A. (2005). Isolation of a fragment homologous to the rp49 constitutive gene of Drosophila in the Neotropical malaria vector Anopheles aquasalis (Diptera: Culicidae). *Memorias Do Instituto*

*Oswaldo Cruz*, *100*(6), 545–547. https://doi.org/10.1590/s0074-02762005000600008

Göertz, G. P., van Bree, J. W. M., Hiralal, A., Fernhout, B. M., Steffens, C., Boeren, S., Visser, T. M., Vogels, C. B. F., Abbo, S. R., Fros, J. J., Koenraadt, C. J. M., van Oers, M. M., & Pijlman, G. P. (2019). Subgenomic flavivirus RNA binds the mosquito DEAD/H-box helicase ME31B and determines Zika virus transmission by Aedes aegypti. *Proceedings of the National Academy of Sciences of the United States of America*, *116*(38), 19136–19144. https://doi.org/10.1073/pnas.1905617116

Gómez-Díaz, E., Jordà, M., Peinado, M. A., & Rivero, A. (2012). Epigenetics of Host-Pathogen Interactions: The Road Ahead and the Road Behind. *PLoS Pathogens*, *8*(11). https://doi.org/10.1371/journal.ppat.1003007

Iyer, N. G., Ozdag, H., & Caldas, C. (2004). p300/CBP and cancer. *Oncogene*, *23*(24), 4225–4231. https://doi.org/10.1038/sj.onc.1207118

Karmodiya, K., Krebs, A. R., Oulad-Abdelghani, M., Kimura, H., & Tora, L. (2012). H3K9 and H3K14 acetylation co-occur at many gene regulatory elements, while H3K14ac marks a subset of inactive inducible promoters in mouse embryonic stem cells. *BMC Genomics*, *13*, 424. https://doi.org/10.1186/1471-2164-13-424

Kirfel, P., Vilcinskas, A., & Skaljac, M. (2020). Lysine Acetyltransferase p300/CBP Plays an Important Role in Reproduction, Embryogenesis and Longevity of the Pea Aphid Acyrthosiphon pisum. *Insects*, *11*(5). https://doi.org/10.3390/insects11050265

Kurdistani, S. K., & Grunstein, M. (2003). Histone acetylation and deacetylation in yeast. *Nature Reviews. Molecular Cell Biology*, *4*(4), 276–284. https://doi.org/10.1038/nrm1075

Li, K.-L., Zhang, L., Yang, X.-M., Fang, Q., Yin, X.-F., Wei, H.-M., Zhou, T., Li, Y.-B., Chen, X.-L., Tang, F., Li, Y.-H., Chang, J.-F., Li, W., & Sun, F. (2018). Histone acetyltransferase CBP-related H3K23 acetylation contributes to courtship learning in Drosophila. *BMC Developmental Biology*, *18*(1), 20. https://doi.org/10.1186/s12861-018-0179-z

Liu, X., Wang, L., Zhao, K., Thompson, P. R., Hwang, Y., Marmorstein, R., & Cole, P. A. (2008). The structural basis of protein acetylation by the p300/CBP transcriptional coactivator. *Nature*, *451*(7180), 846–850. https://doi.org/10.1038/nature06546

Livak, K. J., & Schmittgen, T. D. (2001). Analysis of relative gene expression data using real-time quantitative PCR and the 2(-Delta Delta C(T)) Method. *Methods (San Diego, Calif.)*, *25*(4), 402–408. https://doi.org/10.1006/meth.2001.1262

Mukherjee, S. P., Behar, M., Birnbaum, H. A., Hoffmann, A., Wright, P. E., & Ghosh, G. (2013). Analysis of the RelA:CBP/p300 interaction reveals its involvement in NF-κB-driven transcription. *PLoS Biology*, *11*(9), e1001647. https://doi.org/10.1371/journal.pbio.1001647

Paradkar, P. N., Duchemin, J., Voysey, R., & Walker, P. J. (2014). *Dicer-2-Dependent Activation of Culex Vago Occurs via the TRAF-Rel2 Signaling Pathway*. *8*(4). https://doi.org/10.1371/journal.pntd.0002823

Paschos, K., & Allday, M. J. (2010). Epigenetic reprogramming of host genes in viral and microbial pathogenesis. *Trends in Microbiology*, *18*(10), 439–447. https://doi.org/10.1016/j.tim.2010.07.003

Raisner, R., Kharbanda, S., Jin, L., Jeng, E., Chan, E., Merchant, M., Haverty, P. M., Bainer, R., Cheung, T., Arnott, D., Flynn, E. M., Romero, F. A., Magnuson, S., & Gascoigne, K. E. (2018). Enhancer Activity Requires CBP/P300

Bromodomain-Dependent Histone H3K27 Acetylation. *Cell Reports*, *24*(7), 1722–1729. https://doi.org/10.1016/j.celrep.2018.07.041

Ramirez, J. L., Souza-Neto, J., Torres Cosme, R., Rovira, J., Ortiz, A., Pascale, J. M., & Dimopoulos, G. (2012). Reciprocal Tripartite Interactions between the Aedes aegypti Midgut Microbiota, Innate Immune System and Dengue Virus Influences Vector Competence. *PLOS Neglected Tropical Diseases*, *6*(3), 1–11. https://doi.org/10.1371/journal.pntd.0001561

Rando, O. J., & Verstrepen, K. J. (2007). Timescales of genetic and epigenetic inheritance. *Cell*, *128*(4), 655–668. https://doi.org/10.1016/j.cell.2007.01.023

Reece, S. E., Ramiro, R. S., & Nussey, D. H. (2009). Plastic parasites : sophisticated strategies for survival and reproduction ? *Evolutionary Aplications*, 11–23. https://doi.org/10.1111/j.1752-4571.2008.00060.x

Ren, J., Wen, L., Gao, X., Jin, C., Xue, Y., & Yao, X. (2009). DOG 1.0: illustrator of protein domain structures. In *Cell research* (Vol. 19, Issue 2, pp. 271–273). https://doi.org/10.1038/cr.2009.6

Revilla, Y., & Granja, A. G. (2009). Viral mechanisms involved in the transcriptional CBP/p300 regulation of inflammatory and immune responses. *Critical Reviews in Immunology*, *29*(2), 131–154. https://doi.org/10.1615/critrevimmunol.v29.i2.30

Ribeiro, F. S., de Abreu da Silva, I. C., Carneiro, V. C., Belgrano, F. dos S., Mohana-Borges, R., de Andrade Rosa, I., Benchimol, M., Souza, N. R. Q., Mesquita, R. D., Sorgine, M. H. F., Gazos-Lopes, F., Vicentino, A. R. R., Wu, W., de Moraes Maciel, R., da Silva-Neto, M. A. C., & Fantappié, M. R. (2012). The dengue vector Aedes aegypti contains a functional high mobility group box 1 (HMGB1) protein with a unique regulatory C-terminus. *PloS One*, *7*(7), e40192.

https://doi.org/10.1371/journal.pone.0040192

Ruiz, J. L., Yerbanga, R. S., Lefèvre, T., Ouedraogo, J. B., Corces, V. G., & Gómez-Díaz, E. (2019). Chromatin changes in Anopheles gambiae induced by Plasmodium falciparum infection. *Epigenetics & Chromatin*, *12*(1), 5. https://doi.org/10.1186/s13072-018-0250-9

Sedkov, Y., Cho, E., Petruk, S., Cherbas, L., Smith, S. T., Jones, R. S., Cherbas, P., Canaani, E., Jaynes, J. B., & Mazo, A. (2003). Methylation at lysine 4 of histone H3 in ecdysone-dependent development of Drosophila. *Nature*, *426*(6962), 78–83. https://doi.org/10.1038/nature02080

Shahbazian, M. D., & Grunstein, M. (2007). Functions of site-specific histone acetylation and deacetylation. *Annual Review of Biochemistry*, *76*, 75–100. https://doi.org/10.1146/annurev.biochem.76.052705.162114

Sim, S., Jupatanakul, N., Ramirez, J. L., Kang, S., Romero-Vivas, C. M., Mohammed, H., & Dimopoulos, G. (2013). Transcriptomic profiling of diverse Aedes aegypti strains reveals increased basal-level immune activation in dengue virus-refractory populations and identifies novel virus-vector molecular interactions. *PLoS Neglected Tropical Diseases*, *7*(7), e2295. https://doi.org/10.1371/journal.pntd.0002295

Thompson, J. D., Higgins, D. G., & Gibson, T. J. (1994). CLUSTAL W: improving the sensitivity of progressive multiple sequence alignment through sequence weighting, position-specific gap penalties and weight matrix choice. *Nucleic Acids Research*, *22*(22), 4673–4680. https://doi.org/10.1093/nar/22.22.4673

Tie, F., Banerjee, R., Stratton, C. A., Prasad-Sinha, J., Stepanik, V., Zlobin, A., Diaz, M. O., Scacheri, P. C., & Harte, P. J. (2009). CBP-mediated acetylation of histone H3 lysine 27 antagonizes Drosophila Polycomb silencing. *Development*

*(Cambridge, England)*, *136*(18), 3131–3141. https://doi.org/10.1242/dev.037127

Tikhe, C. V, & Dimopoulos, G. (2021). Mosquito antiviral immune pathways. *Developmental & Comparative Immunology*, *116*, 103964. https://doi.org/https://doi.org/10.1016/j.dci.2020.103964

Vargas, V., Cime-Castillo, J., & Lanz-Mendoza, H. (2020). Immune priming with inactive dengue virus during the larval stage of Aedes aegypti protects against the infection in adult mosquitoes. *Scientific Reports*, *10*(1), 6723. https://doi.org/10.1038/s41598-020-63402-z

Weaver, S. C., Costa, F., Garcia-Blanco, M. A., Ko, A. I., Ribeiro, G. S., Saade, G., Shi, P.-Y., & Vasilakis, N. (2016). Zika virus: History, emergence, biology, and prospects for control. *Antiviral Research*, *130*, 69–80. https://doi.org/10.1016/j.antiviral.2016.03.010

**Author contributions**

A.M.A, I.C.A.S., P.L.O., T. M. V. AND M.R.F. conceived and designed the experiments; A.M.A., I.C.A.S., A.R.R.V., M.A.P., and K.C.M. performed the experiments; L.M.H. prepare and titrate Zika virus stocks; A.M.A, I.C.A.S., V.C.C., O.A.C.T., T. M. V., P.L.O., and M.R.F analyzed the data. A.M.A and M.R.F wrote the paper.

**Funding**

This work was supported by the Conselho Nacional de Desenvolvimento Científico e Tecnológico, CNPq (grant number 470099/20143), Fundação de Amparo à Pesquisa do Estado do Rio de Janeiro, Faperj (grant number E-26/202990/2015) and Instituto Nacional de Ciência e Tecnologia em Entomologia Molecular, INCT-EM, grant number 573959/2008-0).

**Acknowledgements**

We thank Jaciara Miranda Freire for running the insectary and excellent technical assistance with mosquito rearing.

**Figure legends**

Figure 1. Overview of AaCBP protein domain conservation. Schematic representation of the full-length AaCBP protein (XP_011493407.2), depicting the conserved functional domains: the TAZ domain (orange), KIX domain (pink), bromo domain (blue), HAT domain (purple) and CREB domain (green). The full-length CBP from *Homo sapiens* (NP_001420.2), *Apis melifera* (XP_026294861.1) and *Drosophila melanogaster* (AAB53050.1) are also shown for comparison. The percentages of similarity of the CBP-HAT domains are shown within the purple boxes.

Figure 2. ZIKV infection modulates the expression and activity of AaCBP. Aag2 cells as well as mosquitoes were infected with ZIKV at a MOI of 2.0, and 60 PFUs,

respectively. Mosquito infections were performed by intrathoracic injections. The expression of AaCBP in mosquitoes (A-C) or Aag2 cells (D) was measured by qRT-PCR on the indicated tissues and days post infection. E and F. Western blot of total protein extract from Aag2 cells infected with ZIKV virus, or mock-infected at different time points. Monoclonal antibodies against H3K9ac, H3K27ac, H3 panacetylated (Panac), or H3 (as a loading control) were used. The intensity of the bands was quantified by densitometry analysis plotted as a graph using ImageJ (NIH Software). Western blotting was performed on 3 independent biological replicates and one representative is shown here. Error bars indicate the standard error of the mean; statistical analyses were performed by Student's *t* test. *, $p < 0.05$; **, $p < 0.01$.

Figure 3. *AaCBP* gene knockdown compromises the lifespan of ZIKV-infected mosquitoes. A. One hundred adult female mosquitoes were injected intrathoracically with double-stranded RNAs for the AaCBP or Luc control gene, two days before Zika infections (by intrathoracic injections). Survival of the mosquitoes was monitored on a daily basis, until Day 20. B. Survival curve of mosquitoes that were not injected, mock-infected mosquitoes that were injected with for dsLuc or dsAaCBP, and mosquitoes that were injected with for dsLuc or dsAaCBP and infected with ZIKV. C and D. Midguts or fat bodies from silenced mosquitoes were assessed for virus infection intensity at different time points. Each dot or square represents the mean plaque-forming units (PFUs) per two midguts or fat bodies (totaling 20 midguts or fat bodies examined) from five independent experiments. Bars indicate the standard error of the mean; tatistical analyses were performed by Student's *t* test. *, $p < 0.05$; **, $p < 0.01$.

Figure 4. The expression of antiviral immune-response genes is reduced in ZIKV-infected mosquitoes silenced for AaCBP. A and B. Fifty adult female mosquitoes were silenced for AaCBP, and after two days, mosquitoes were infected with ZIKV. The expression of cecropin D, cecropin G, attacin, serpin, defensing C, Dicer 2, Argonaut 2 and vago 2 in the midgut (A) or fat body (B) was measured by qRT-PCR four days post infection. Silencing levels of AaCBP in both tissues are shown (first bars in Panels A and B). qRT-PCR was performed from 3 independent biological replicates. Bars indicate the standard error of the mean; statistical analyses were performed by Student's *t* test. *, $p < 0.05$.

Figure 5. Histone hyperacetylation in ZIKV-infected mosquitoes induces immune responses and suppresses virus infection. A-E. Fifty adult female mosquitoes were infected with ZIKV and treated with 0.5 M NaB for three days. A-C. The expression of defensin A, defensin C, and cecropin D, in whole mosquito tissues was measured by qRT-PCR. qRT-PCR was performed on 3 independent biological replicates. D and E. Midguts or fat bodies from ZIKV-infected mosquitoes treated with NaB were assessed for infection intensity at 3 or 7 days post infection. Bars indicate the standard error of the mean; statistical analyses were performed by Student's *t* test. *, $p < 0.05$; **, $p < 0.01$.

Figure 6. Proposed model for the role of AaCBP-mediated histone acetylation in suppressing ZIKV infection in *A. aegypti*. Zika infection signals the functional activation of transcription factors (TF) that translocate to the nucleus where they activate the expression of immune-related genes to fight the virus infection. Chromatin decondensation is mandatory for gene activation. Therefore, AaCBP is

likely recruited by TFs to target promoters, where it exerts its histone acetyltransferase activity, leading to an open state of the chromatin at these promoter sites.

Supplementary Table 1. List of primers used in this study.

Supplementary Figure 1. Protein domain and alignment of putative histone acetyltransferases from *A. aegypti*. A. Genome identification of putative lysine acetyltransferase (KAT) homologs from *A. aegypti*, AaHAT1 (XP_001651817.1), AaTip60 (XP_021706851.1), AaMOF1 (XP_001658578.2), AaMOF2 (XP_021711683.1), HBO1 (XP_021701314.1), GCN5 (XP_0016566424.1) and AaCBP itself. Functional domains are indicated above each box. B. Protein sequence alignment of the HAT domains from the putative *A. aegypti* KATs. Amino acids in red show identity or conservation among all 7 HAT domains.

Supplementary Figure 2. Blood meal upregulates the expression of AaCBP. Mosquitoes were fed with blood over different time courses and mRNA quantification by qPCR was performed in the midgut or fat body. The results in A and B are pools of at least 3 independent experiments, plotted using samples from sugar-fed mosquitoes as reference. Error bars indicate the standard error of the mean; statistical analyses were performed by Student's *t* test. *, $p < 0.05$; **, $p < 0.01$; ***, $p < 0.001$.

Supplementary Figure 3. Silencing levels of AaCBP after a sugar or blood meal. Two days after feeding, the *AaCBP* gene was knocked down and its expression was measured two days after silencing. qRT-PCR was performed from 3 independent

biological replicates. Bars indicate the standard error of the mean; statistical analyses were performed by Student's *t* test. **, $p < 0.01$.

Supplementary Figure 4. Silencing of AaCBP in adult female mosquitoes by intrathoracic injections of dsRNAs. The expression (A) and activity (B) of AaCBP were used to evaluate the efficiency of gene knockdown. A. The mRNA levels of AaCBP in the midgut, ovary, fat body or whole mosquito were quantified by qRT-PCR at 48 h postinjection with dsCBP or dsLuc. Silencing level was determined by the ratio between mRNA levels of AaCBP-silenced versus dsLuc-injected mosquitoes. B. Western blot of 10 μg of total protein extract of dsCBP- or dsLuc-injected-mosquitoes. Monoclonal antibodies against acetylated- or nonacetylated histone H3 (loading control) are indicated. The intensity of the bands was quantified by densitometry analysis plotted as a graph using ImageJ (NIH Software). Western blotting was performed on 3 independent biological replicates and one representative is shown here. Bars indicate the standard error of the mean; statistical analyses were performed by Student's *t* test. *, $p < 0.05$.

Supplementary Figure 5. ZIKV infection upregulates the expression of antimicrobial peptides in the midgut of *A. aegypti*. Fifty adult female mosquitoes were infected with ZIKV after feeding on infected blood and the expression of cecropin D, cecropin G, attacin, gambicin, serpin and defensin C was measured by qRT-PCR four days post infection. qRT-PCR was performed from 3 independent biological replicates. Bars indicate the standard error of the mean.

Supplementary Figure 6. Silencing of AaCBP is sustainable and efficient until five days of ZIKV infection. Fifty adult female mosquitoes were infected with ZIKV for 1, 5, 7 or 10 days and the expression levels of AaCBP, cecropin G, defensin or vago in the fat body were measured by qRT-PCR on 3 independent biological replicates. Bars indicate the standard error of the mean; statistical analyses were performed by Student's *t* test. *, $p < 0.05$.

Supplementary Figure 7. Histone deacetylase inhibition leads to histone hyperacetylation in *A. aegypti*. Ten adult female mosquitoes were intrathoracically injected with PBS, 0.25 M (17.5 pmol), or 0.5 M (35 pmol) of sodium butyrate (NaB). Four days after treatment, 10 μg of total protein extract from 10 mosquitoes was used for histone acetylation analysis. Western blotting with monoclonal antibodies against H3K9ac, H3K27ac, H3 panacetylated, or H3 (as loading control) was performed. The intensity of the bands was quantified by densitometry (lower panel) analysis plotted as a graph using ImageJ (NIH Software). Western blotting was performed on 3 independent biological replicates and one representative is shown in panel A. Error bars in Panel B indicate the standard error of the mean; statistical analyses were performed by Student's *t* test. *, $p < 0.05$.

CBP/p300

2828 aa

*Aedes aegypti* (XP_0011493407.2)

2414 aa

*Homo sapiens* (NP_001420.2)

2667 aa

*Apis mellifera* (XP_026294861.1)

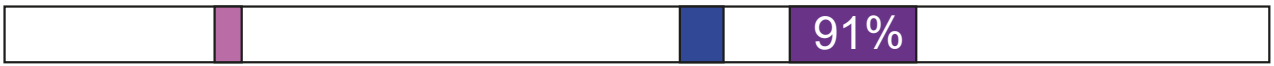


3190 aa

*Drosophila melanogaster* (AAB53050.1)

TAZ KIX Bromo

HAT CREB

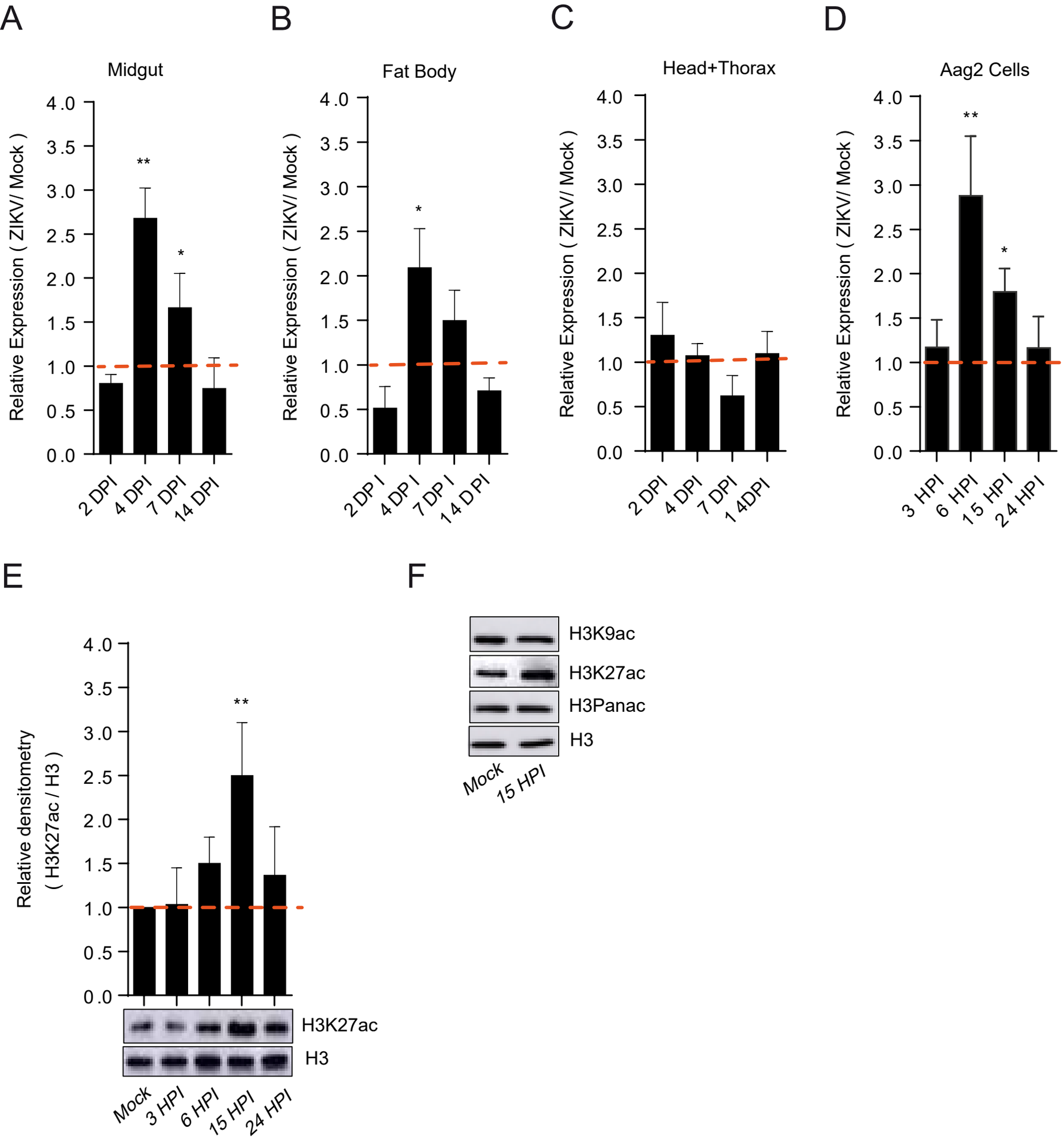
A
Midgut
Relative Expression ( ZIKV/ Mock )
4.0
3.5
3.0
2.5
2.0
1.5
1.0
0.5
0.0
**
*
2 DPI
4 DPI
7 DPI
14 DPI
B
Fat Body
Relative Expression ( ZIKV/ Mock )
*
2 DPI
4 DPI
7 DPI
14 DPI
C
Head+Thorax
Relative Expression ( ZIKV/ Mock )
2 DPI
4 DPI
7 DPI
14DPI
D
Aag2 Cells
Relative Expression ( ZIKV/ Mock )
**
*
3 HPI
6 HPI
15 HPI
24 HPI
E
Relative densitometry
( H3K27ac / H3 )
**
H3K27ac
H3
Mock
3 HPI
6 HPI
15 HPI
24 HPI
F
H3K9ac
H3K27ac
H3Panac
H3
Mock
15 HPI

A

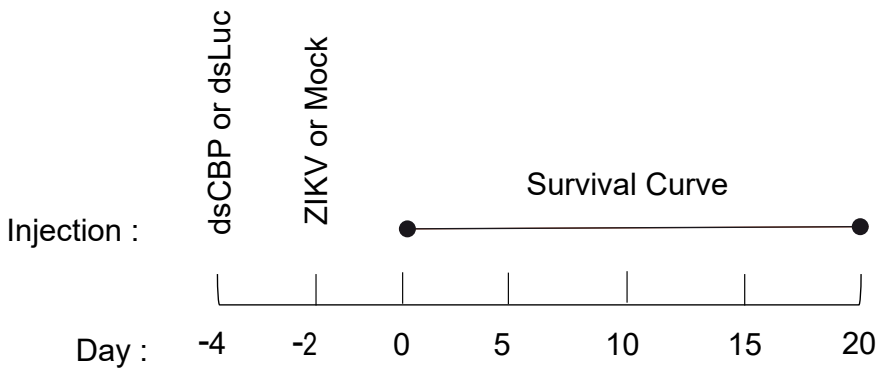
dsCBP or dsLuc
ZIKV or Mock
Survival Curve
Injection :
Day :
-4
-2
0
5
10
15
20

B

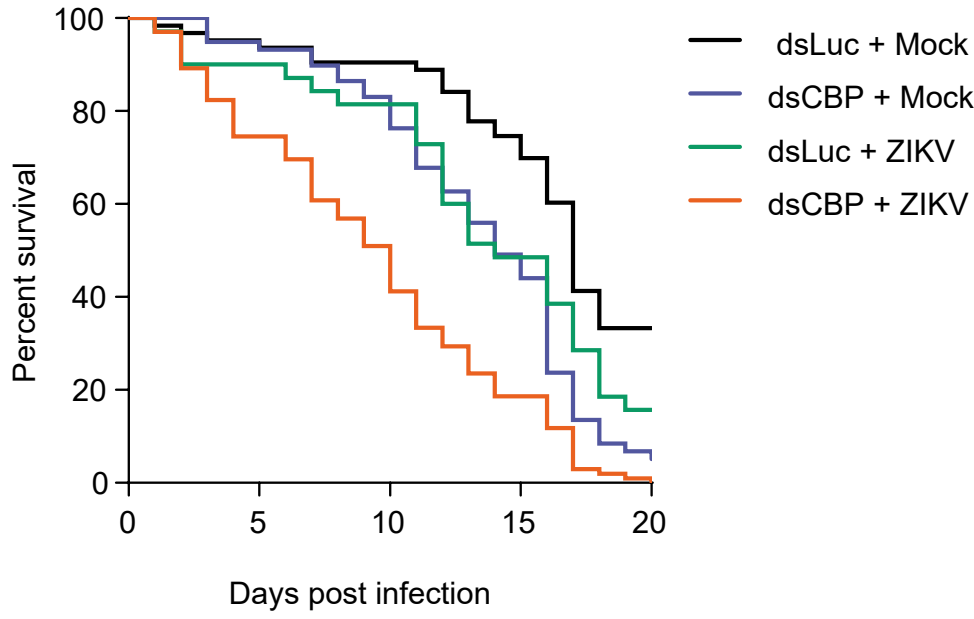
Percent survival
100
80
60
40
20
0
0
5
10
15
20
Days post infection
dsLuc + Mock
dsCBP + Mock
dsLuc + ZIKV
dsCBP + ZIKV

C

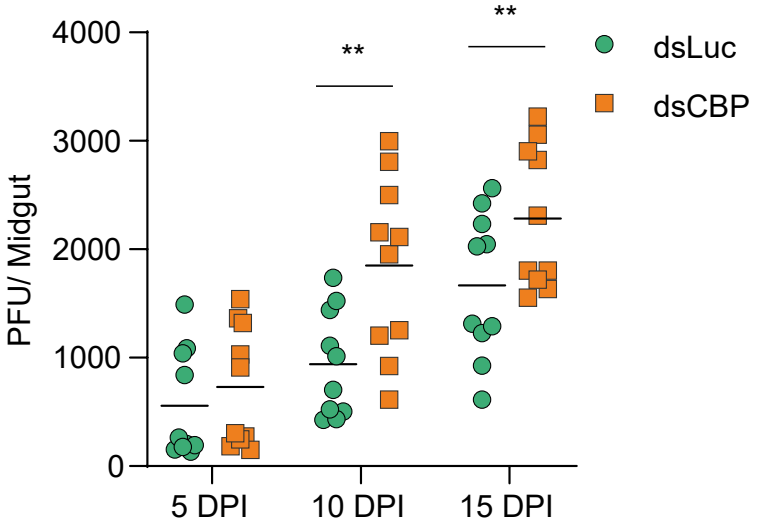
PFU/ Midgut
4000
3000
2000
1000
0
**
**
5 DPI
10 DPI
15 DPI
dsLuc
dsCBP

D

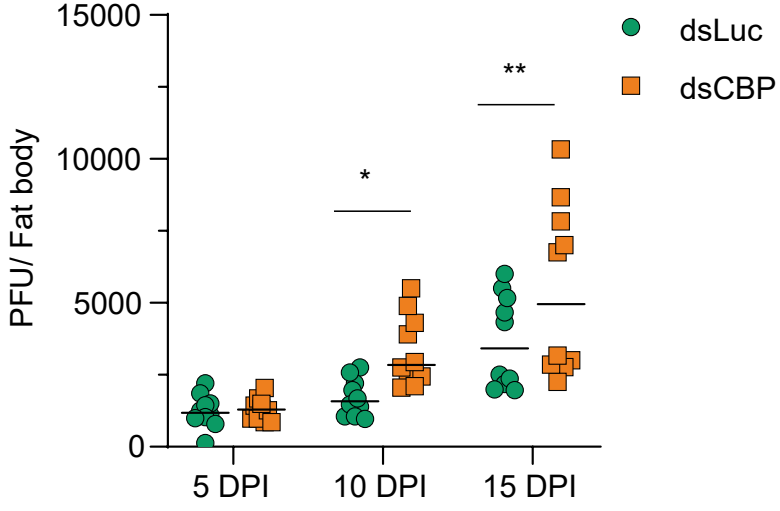
PFU/ Fat body
15000
10000
5000
0
*
**
5 DPI
10 DPI
15 DPI
dsLuc
dsCBP

A

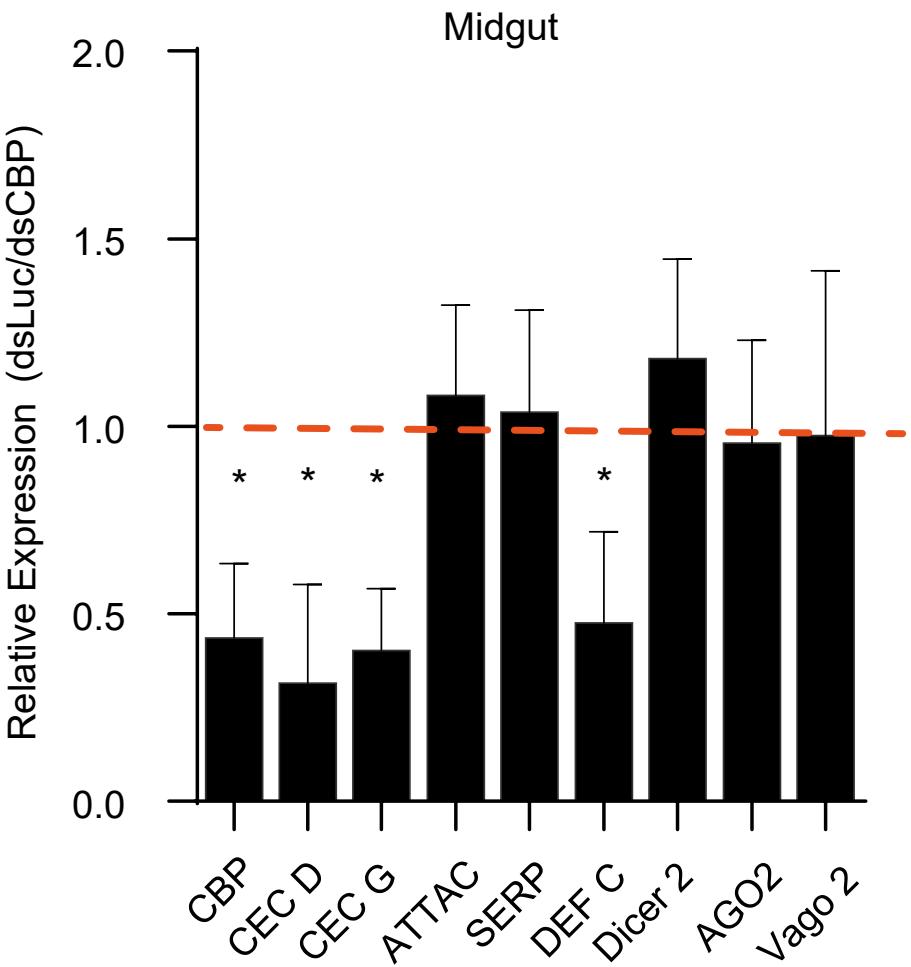
Midgut
Relative Expression (dsLuc/dsCBP)
2.0
1.5
1.0
0.5
0.0
*
*
*
*
CBP
CEC D
CEC G
ATTAC
SERP
DEF C
Dicer 2
AGO2
Vago 2

B

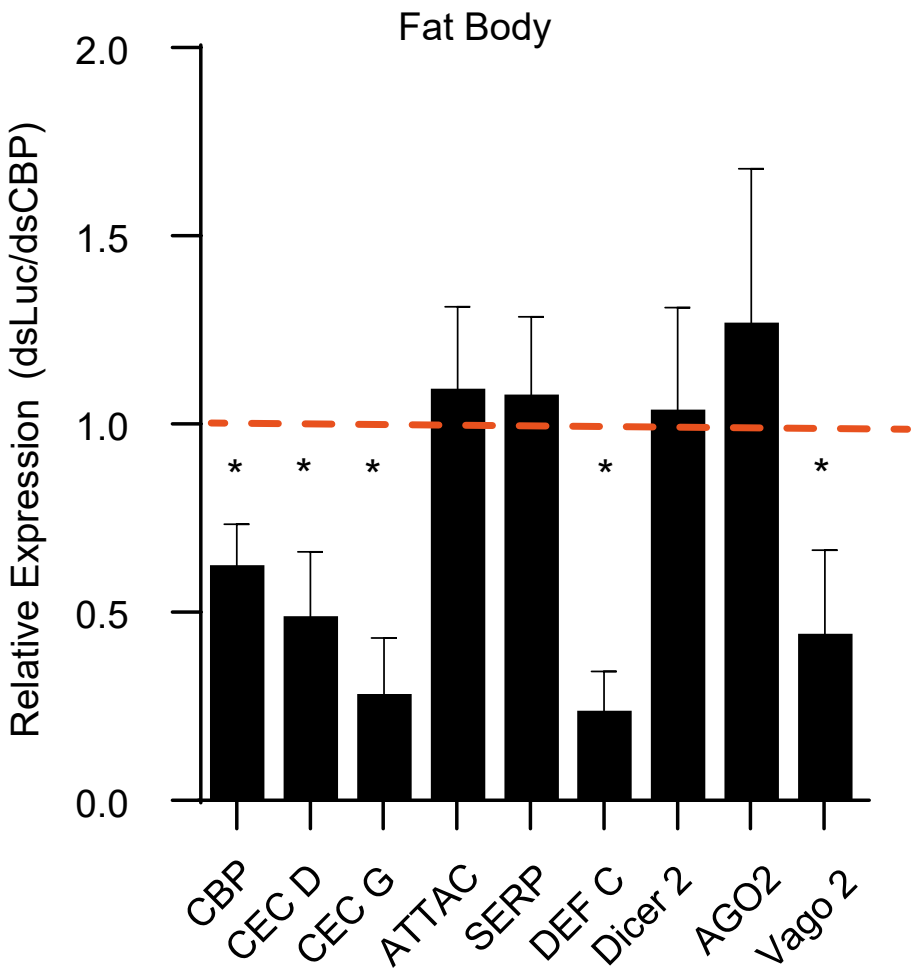
Fat Body
Relative Expression (dsLuc/dsCBP)
2.0
1.5
1.0
0.5
0.0
*
*
*
*
*
CBP
CEC D
CEC G
ATTAC
SERP
DEF C
Dicer 2
AGO2
Vago 2

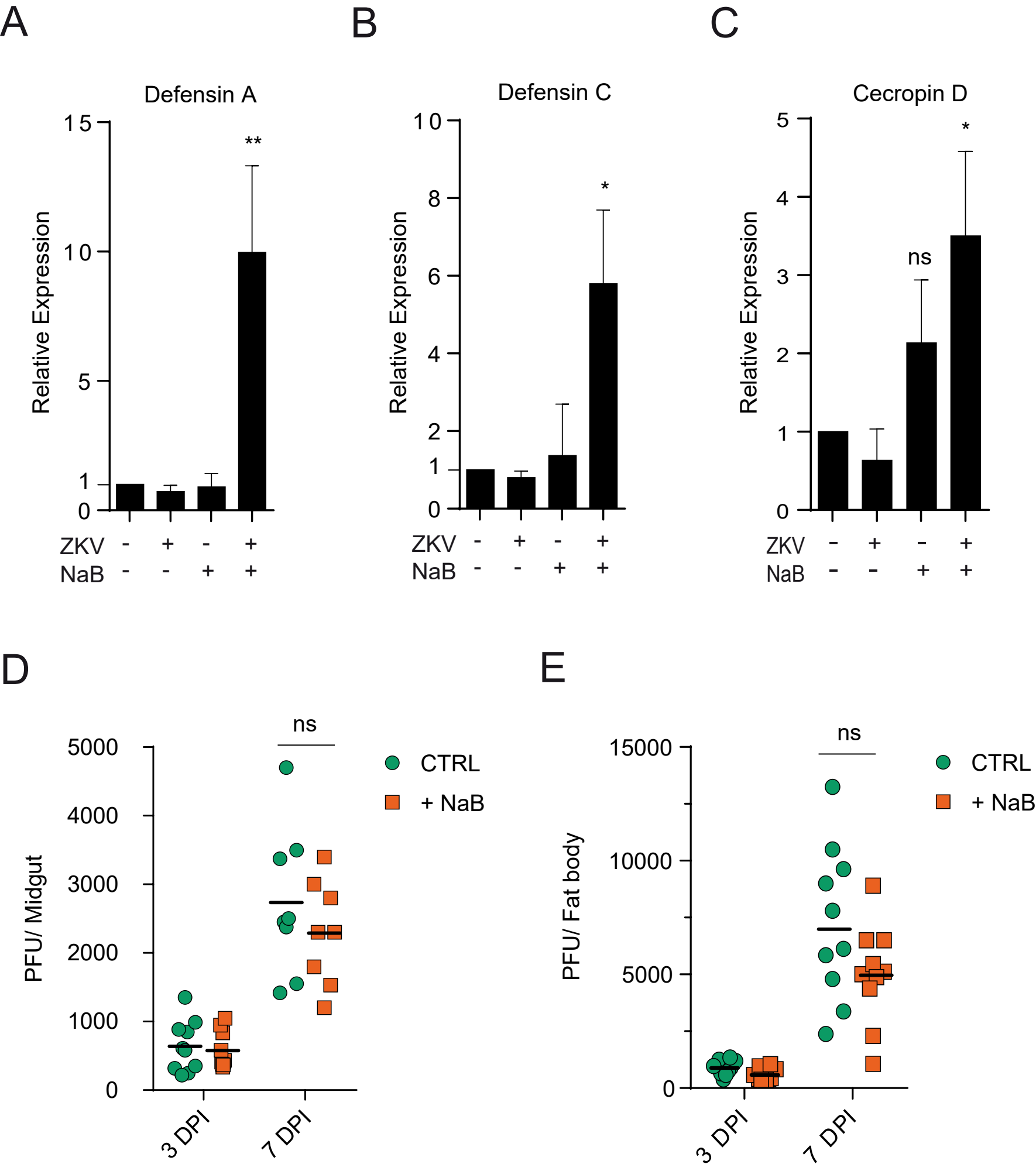
A
Defensin A
Relative Expression
15
10
5
1
0
**
ZKV - + - +
NaB - - + +
B
Defensin C
Relative Expression
10
8
6
4
2
1
0
*
ZKV - + - +
NaB - - + +
C
Cecropin D
Relative Expression
5
4
3
2
1
0
ns
*
ZKV - + - +
NaB - - + +
D
PFU/ Midgut
5000
4000
3000
2000
1000
0
ns
CTRL
+ NaB
3 DPI
7 DPI
E
PFU/ Fat body
15000
10000
5000
0
ns
CTRL
+ NaB
3 DPI
7 DPI

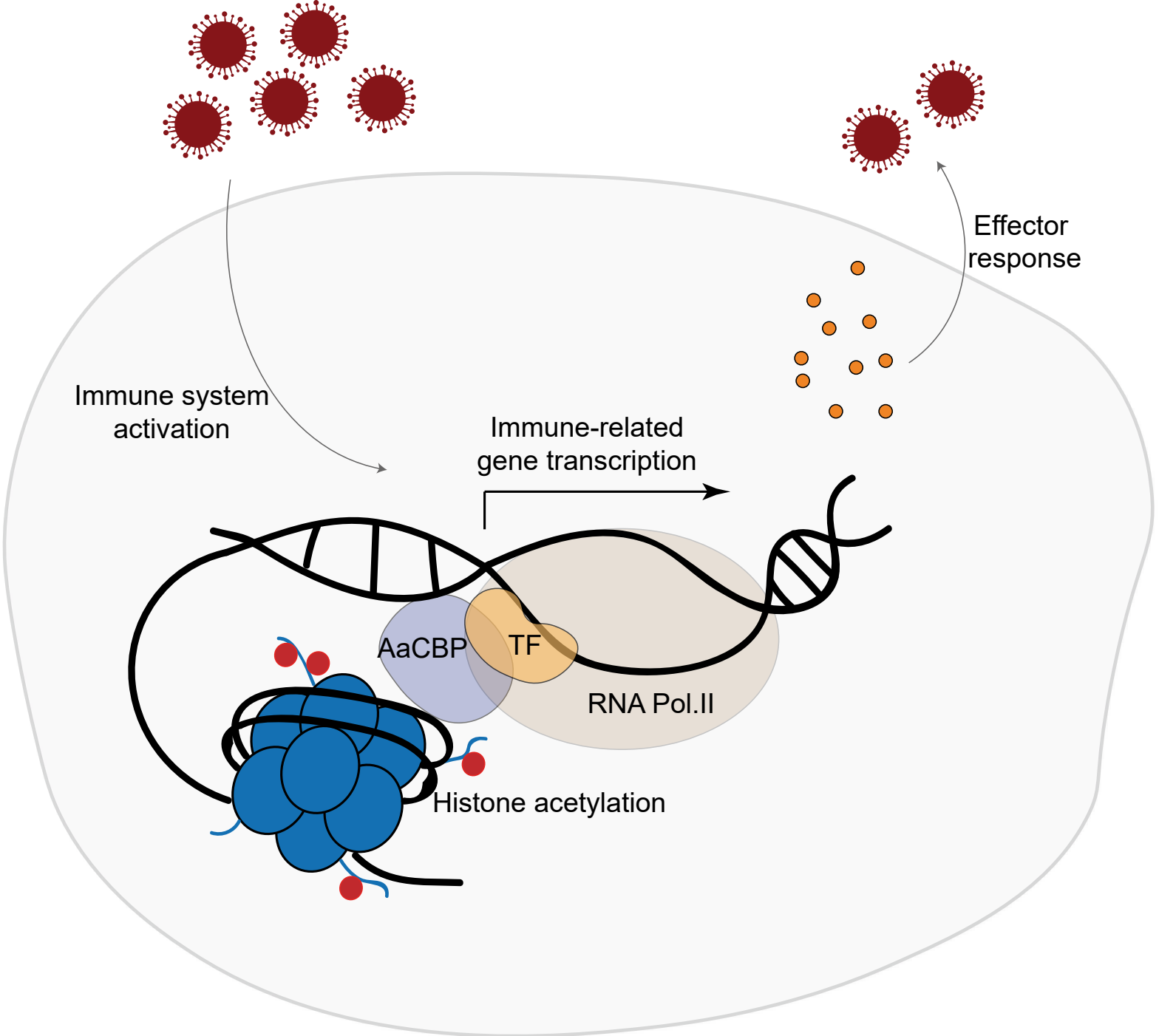
Effector
response
Immune system
activation
Immune-related
gene transcription
AaCBP
TF
RNA Pol.II
Histone acetylation